ACS Macro Letters

pubs.acs.org/macroletters Letter

Toward Plant Cyborgs: Hydrogels Incorporated onto Plant Tissues Enable Programmable Shape Control

Jiayu Zhao, Yifeng Ma, Nicole F. Steinmetz,* and Jinhye Bae*

Cite This: ACS Macro Lett. 2022, 11, 961−966 Read Online

ACCESS | Metrics & More | Article Recommendations | Supporting Information

ABSTRACT: Engineered living materials (ELMs) that incorporate living organisms and synthetic materials enable advanced functional properties. Here, we seek to create plant cyborgs by combining plants or plant tissues with stimuli-responsive polymeric materials. Plant tissues with integrated shape control may find applications in regenerative medicine, and the shape control of living plants enables another dimension of adaptability and response to environmental threats, which can be applied to next-generation precision farming. In this work, we develop chemistry to integrate stimuli-responsive poly(*N*-isopropylacrylamide) (PNIPAM) hydrogels with decellularized plant tissues assisted by 3D printing. We demonstrate programmable shape morphing in response to thermal cues and ultraviolet (UV) light. Specifically, by taking advantage of the extrusion-based 3D printing method, we deposit nanocomposite PNIPAM precursors onto silane-treated decellularized leaf surface with prescribed shapes and spatial control. When subjected to external stimuli, the strain mismatch generated between the swellable nanocomposite PNIPAM and nonswellable decellularized leaf enables folding and bending to occur. This strategy to integrate the plant tissues with stimuli-responsive hydrogels allows the control of leaf morphology, opening avenues for plant-based biosensors and soft actuators to enhance food security; such materials also may find applications in biomedicine as tissue-engineering scaffolds.

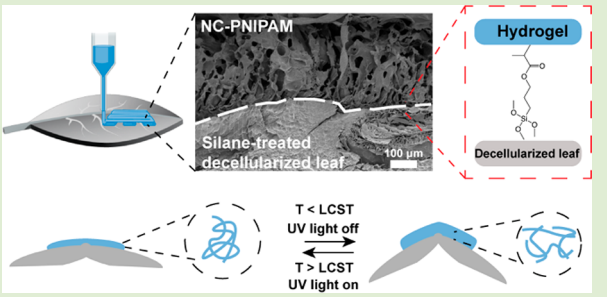

The emerging field of ELMs aims to produce smart materials that can respond and adapt to environmental changes, that can self-heal, and that can perform these tasks dynamically and autonomously. This is achieved by integrating living biological systems with synthetic materials,[1,2] thereby opening new avenues in applications such as biosensors,[3] remediation,[4] and soft robotics.[5] The living cells or tissues are generally engineered through genetic modification, chemical functionalization, or simply doped with synthetic materials to produce the desired properties.

Plants as complex biological systems exemplify what nature is capable of generating from spores or seeds to highly ordered hierarchical structures that can adapt to the external environment in a spatiotemporal manner.[6] Endeavors toward developing plant-based materials with new functionalities have been made in the past several years.[6,7] Specifically, the Berggren group reported electronic plants by incorporating electrically conductive polymers into the internal structure of plants.[8] The Strano group showed plant-based photonics by infiltrating nanoparticles to plant mesophyll.[9] The Appel group demonstrated fire prevention in high-risk landscapes through spray application of cellulose-based viscoelastic fluid on vegetation.[10] Chen et al. developed a Venus flytrap-based soft actuator by modulating the flytrap's electrophysiology using a conformable electrode consisting of hydrogel/gold nanomesh elastomer composite.[11] Despite the recent advances, it is still challenging to create plant-based materials that can transform into programmable shapes in response to external stimuli with spatial and temporal precision.

The long-term goal for our project is to endow the living plants with programmable shape control in response to environmental cues by the incorporation of stimuli-responsive hydrogels. Ultimately, it could serve as a platform for the biosensor to reflect plants' health and monitor their growth. To begin with, we have studied the decellularized plant tissues, which have drawn much attention recently as substitutes for animal tissues, due to their lower cost, higher accessibility,[12] biocompatibility, and environmentally friendly processing procedures.[13] Moreover, the plant's native vascular structure follows Murray's law, matching the mammalian tissue hierarchy.[14] With the network essential to gas and nutrients transport, a wide range of mammalian cell lines can attach to the decellularized plant tissue with high survival rate.[13,15] Gershlak et al. successfully demonstrated the potential of decellularized plants as scaffolds for tissue engineering by recellularized the decellularized spinach leaves with human

Received: May 11, 2022
Accepted: July 7, 2022

https://doi.org/10.1021/acsmacrolett.2c00282
ACS Macro Lett. 2022, 11, 961−966

endothelial cells.[16] The Pelling group showed that the decellularized apple tissue can be used as a 3D cellulose scaffold for culturing mammalian cells in vitro.[17] Furthermore, this group also reported that the cell attachment and invasion can be improved by casting collagen hydrogel onto the decellularized apple tissue scaffold.[18] Thus, there is a large potential of plant tissue ELMs as a platform for biosensors and soft actuators.

In this work, we report a strategy to create adhesion at the interface of the plant-synthetic polymer that enables programmable shape-morphing in response to temperature and UV light. A hydrogel is a three-dimensional (3D) network consisting of cross-linked hydrophilic polymers that can retain a large amount of water. Among these, PNIPAM is a well-known temperature-responsive hydrogel that possesses lower critical solution temperature (LCST) around 32 °C,[19] which is a safe actuation temperature that would not damage the plants. The addition of nanoparticles to PNIPAM-based hydrogels allows us to readily tune the rheological properties to enable extrusion-based 3D printing[20] and endows the PNIPAM nanocomposite hydrogels with responsiveness to various stimuli.[21] In addition, the LCST can be shifted with a range around 20−50 °C by further changing its composition, pH and ionic strength,[22] offering a wide range of temperature control to fulfill different usage scenarios. The plant-based soft actuator is prepared by patterning the nanocomposite PNIPAM onto the surfaces of decellularized leaves via extrusion-based 3D printing. Upon immersing the decellularized leaf/nanocomposite PNIPAM bilayer structure in a water bath at 22 °C, the strain-mismatch generated between the swellable nanocomposite hydrogel and nonswellable decellularized leaves led to the shape transformation (i.e., folding or bending). We note that this phenomenon is reversible due to the reversible swelling and deswelling of the nanocomposite PNIPAM as the temperature is below or higher than LCST, respectively. The incorporation of graphene oxide (GO) within the nanocomposite PNIPAM further enables remote light responsiveness owing to the photothermal effect of GO,[21] where it serves as a local heater within the PNIPAM to raise the temperature above LCST, resulting in the deswelling of the PNIPAM network. As a proof-of-concept, we demonstrate the programmable shape morphing behavior using two kinds of nanocomposite PNIPAM hydrogels, which are nanoclay (NC)-PNIPAM and GO-NC-PNIPAM, that possess temperature and light responsiveness by external stimuli, respectively. We anticipate that the concept and strategy employed in this work to create plant-based shape morphing actuators will further push the development of plant cyborgs in living systems.

Spinacia oleracea (spinach) was chosen as our model plant because they are readily available, soft, flat (i.e., low curvature), and have smooth surfaces without hairy structures, which can facilitate printing and attachment of the hydrogels due to the better contact compared to the ones with hairy surfaces. Spinach leaves were obtained from local grocery stores were decellularized using sodium dodecyl sulfate (SDS) and bleach treatment, adapted from previously reported methods.[16] Leaves became translucent after 5 days of immersing in 10 wt % SDS in Millipore water and then became transparent with additional 5−7 days of immersion in the mixture of 0.1% triton X-100 and 1% bleach solution (Figure 1A). We note that one of the benefits of using decellularized leaves is that the mechanical properties can be readily controlled by varying the

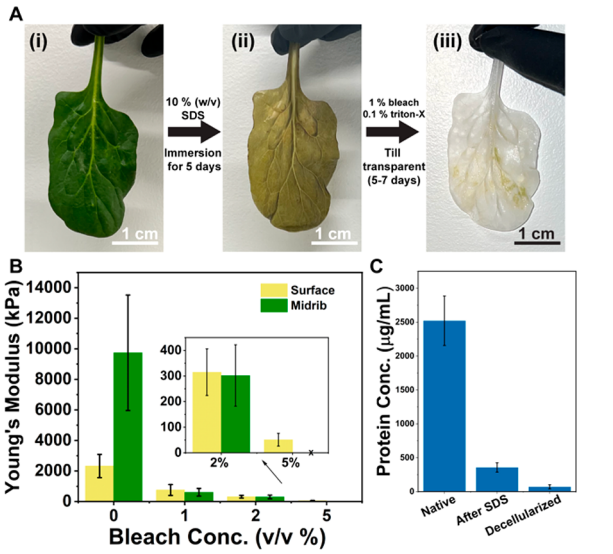

Figure 1. (A) Decellularization process of (i) native spinach leaf, (ii) soaking in 10% (w/v) SDS solution after 5 days, followed by soaking in the mixture of triton X-100 and bleach solution; (B) Young's modulus of the surface (yellow) and midrib (green) of the decellularized leaves after soaking in bleach solution with different concentrations varying from 0 to 5% (v/v). (C) Protein concentration was quantified using a bicinchoninic acid (BCA) protein assay.

bleach concentration. The Young's modulus of the surface of the leaves decreased 2 orders of magnitude (2373 to 51 kPa) by increasing the bleach concentration from 0 to 5% (v/v; Figure 1B). Through optimization, we chose 1% (v/v) bleach concentration, because it reproducibly yielded decellularized leaves with Young's modulus of 758 kPa (Figure 1B), which is not only strong enough to maintain the structural integrity but also soft enough to be deformed. To evaluate the decellularization process, we carried out a BCA assay using pulverized leaves resuspended in 10 mM potassium phosphate buffer to quantify the protein concentration in each step. It shows that the protein content decreased significantly from 2520.8 ± 364.6 μg/mL per gram of native leaves to 356.3 ± 68.3 μg/mL per gram after soaking in SDS and further decreased to 70.5 ± 29.9 μg/mL per gram after decellularization (Figure 1C), which proves that the decellularization process was successful.

The nanocomposite hydrogel precursor consists of NIPAM as the monomer, *N*,*N*′-methylenebis(acrylamide) (BIS) as a cross-linker, Irgacure 2959 as a photoinitiator, and NC as a rheological modifier. NC is a two-dimensional (2D) disc with ∼25 nm diameter and ∼1 nm thickness. The positively charged edges and negatively charged surfaces of NC discs allow them to form a so-called "house-of-cards" structure through electrostatic attraction upon dispersion in water,[23] which endows the NC-PNIPAM precursor ink with shear-thinning property (Figure 2A) and solid-like behavior (storage modulus G' > loss modulus G'') (Figure 2B). Although the addition of GO slightly decreases the viscosity and G', the shear-thinning property (Figure 2A) and solid-like behavior (Figure 2B) are preserved for GO-NC-PNIPAM precursor ink. The programmable leaf-based soft actuator is created by patterning the nanocomposite PNIPAM hydrogels and the decellularized leaves into a bilayer structure using extrusion-based 3D printing,[24] where the nanocomposite PNIPAM precursor ink was deposited onto the decellularized leaf surface and printed

https://doi.org/10.1021/acsmacrolett.2c00282
ACS Macro Lett. 2022, 11, 961−966

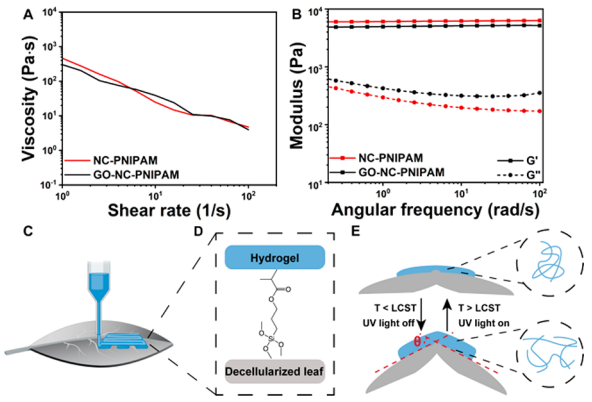

Figure 2. Log−log plots of (A) viscosity as a function of shear rate and (B) modulus as a function of angular frequency of NC-PNIPAM and GO-NC-PNIPAM precursor inks; (C) Schematic of depositing hydrogel precursor ink onto the decellularized leaf surface using extrusion-based 3D printing in perspective view; (D) Schematic of the adhesion mechanism; (E) Schematic of the reversible shape morphing in response to temperature and UV light change in side-view, with a folding angle of θ at equilibrium state. The schematic is created with BioRender.com.

into the prescribed shape at the desired location (Figure 2C). We note that the decellularized leaves were treated with functional silane 3-(trimethoxysilyl) propyl methacrylate (TMSPMA) before 3D printing of the nanocomposite PNIPAM precursor to allow the formation of a self-assembled layer of TMSPMA, as assisted by hydrogen bonding between the silane and the hydroxyl groups on the surfaces of decellularized leaves.[25] After 3D printing, the bilayer structure of the nanocomposite PNIPAM precursor/decellularized leaf was transferred to a homemade humidity box and exposed to UV light irradiation (253 mW/cm^2, 142 s) to photo-cross-link the PNIPAM precursor. During the photo-cross-linking, the methacrylate terminal group of TMSPMA copolymerized with the acrylate group of PNIPAM under the free radical polymerization process, creating covalent bonds that ensures strong adhesion between the decellularized leaf and the nanocomposite PNIPAM hydrogel layer, which is the essential requirement for the shape morphing process (Figure 1D). When immersing the decellularized leaf/nanocomposite PNIPAM bilayer structure at a temperature below LCST (i.e., 23 °C), the PNIPAM hydrogel swells (i.e., expansion in volume) by absorbing water. Thus, the strain mismatch between the swelled PNIPAM and nonswelled decellularized leaf leads to out-of-plane deformation. On the other hand, increasing the temperature above LCST (i.e., 45 °C) results in the flattening of the bilayer structure due to the deswelling of hydrogels, yielding a shrinkage in volume because the polymer network collapses and expels water.[19] Due to the photothermal effect of GO, the out-of-plane deformation and flattening process can also be controlled by turning off and on the UV light, respectively, in which GO absorb UV and convert it to heat. We note that this process is reversible by adjusting the temperature above and below LCST or by turning on and off UV, respectively (Figure 2E).

To characterize the adhesion between the silane-treated decellularized leaf and the nanocomposite PNIPAM hydrogels, we carried out cross-sectional scanning electron microscopy (SEM) to visualize their interface. The nanocomposite PNIPAM hydrogels on the silane-treated decellularized leaves were first swelled for 24 h to reach the equilibrium state and the bilayer structures were then freeze-dried for preparation of SEM imaging. We note that the nanocomposite hydrogel layer of samples without silane treatment was fully delaminated from the decellularized leaves surface, thus we were unable to image the interface using SEM. The SEM images of NC-PNIPAM/silane-treated decellularized leaf (Figure 3A) and GO-NC-PNIPAM/silane-treated decellularized leaf (Figure 3B) show the seamless contact between these materials, where the top layer exhibits a typical porous hydrogel network due to the water-to-ice transformation.[26] Notably, the distinct interfaces between the hydrogels and silane-treated decellularized leaves exhibit that the hydrogel precursor inks did not penetrate into the decellularized leaves. These conformal and close contact interfaces imply strong adhesion was achieved between the nanocomposite PNIPAM hydrogels and the silane-treated decellularized leaves. Furthermore, to quantify the adhesion, we conducted the lap shear test for the as-prepared nanocomposite hydrogel/decellularized leaves to measure the adhesion strength.[27] The saline-treated decellularized leaves were cut to rectangular strips (8 × 35 × 0.1 mm^3), and NC-PNIPAM and GO-NC-PNIPAM were 3D printed into the rectangular shapes (8 × 35 × 0.4 mm^3) on the surfaces of saline-treated decellularized leaves such that they have an overlapped area in the middle (Figure 3C). As a result, all of the samples tested broke due to the failure of either the decellularized leaves or the nanocomposite hydrogels rather than at the interface. Thus, the adhesion strength is higher than the maximum strength at the break value shown on the stress−strain curve, which is 76 ± 7 and 102 ± 13 kPa for NC-PNIPAM and GO-NC-PNIPAM, respectively (Figure 3D). We note that the mechanical properties are different for the NC-PNIPAM hydrogel at swelled and deswelled state.[28,29] To quantify this, we conducted tensile tests for the NC-PNIPAM in swelled state at 22 °C, deswelled state at 45 °C, and as-prepared state at 22 °C (i.e., before immersing in water). The maximum strength for each condition is 19 ± 4, 136 ± 5, and 103 ± 22 kPa, respectively (Figure S1). The lap-shear tests conducted for the as-prepared state of NC-PNIPAM/

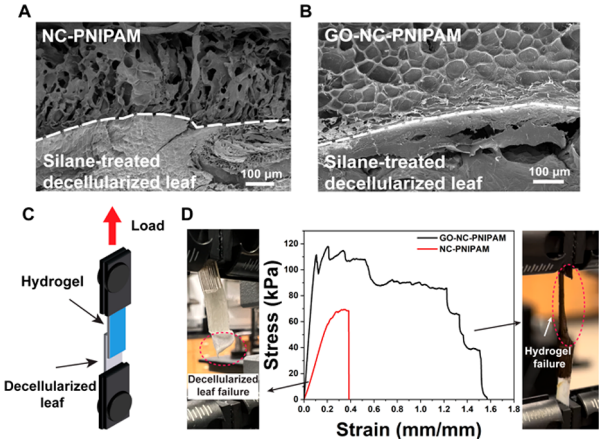

Figure 3. SEM images of the interface between (A) NC-PNIPAM and silane-treated decellularized leaf; and (B) GO-NC-PNIPAM hydrogel and silane-treated decellularized leaf; (C) Schematic of the lap shear test setup; (D) Stress−strain curves of the as-prepared NC-PNIPAM and GO-NC-PNIPAM on silane-treated decellularized leaves during lap shear test. Photographs of the failure of the bilayer structure with NC-PNIPAM (left) and GO-NC-PNIPAM (right).

https://doi.org/10.1021/acsmacrolett.2c00282
ACS Macro Lett. 2022, 11, 961−966

decellularized leaves shown in Figure 3D indicate that the decellularized leaves broke first while the bilayer section remains intact. Thus, the results of tensile tests and lap-shear tests demonstrate that the as-prepared NC-PNIPAM possesses a higher maximum strength (103 ± 22 kPa) than the decellularized leaves (76 ± 7 kPa), and the adhesion strength is greater than the as-prepared NC-PNIPAM strength (103 ± 22 kPa). The swelled NC-PNIPAM possesses the lowest strength value due to the high content of water, whereas the deswelled state possesses the highest strength due to the collapsed polymer networks. The as-prepared NC-PNIPAM exhibits similar maximum strength with the deswelled state. Furthermore, no delamination was observed between the hydrogels (i.e., NC-PNIPAM and GO-NC-PNIPAM) and silane-treated decellularized leaves during multiple cycles of the swelling/deswelling process, and both hydrogels/silane-treated decellularized leaves showed cohesive failure rather than adhesive failure in the lap-shear tests (Figure 3D). Therefore, the adhesion strength for the NC-PNIPAM/silane-treated decellularized leaves at swelled and deswelled states are greater than the maximum strength of NC-PNIPAM at swelled and deswelled states, 19 ± 4 and 136 ± 5 kPa, respectively.

After confirming strong adhesion between the nanocomposite hydrogels and silane-treated decellularized leaves, we demonstrate shape morphing of the decellularized leaf/nanocomposite PNIPAM bilayer structure. Upon swelling, strain mismatches between the hydrogel and leaf scaffold are induced—therefore, programmable shape morphing can be spatially programmed by use of the 3D printing and placement of the nanocomposite hydrogels on the decellularized leaf. As a proof-of-concept, we printed the NC-PNIPAM next to and across the midrib of the cut silane-treated decellularized leaves. The area of the cut as well as the location of the printed NC-PNIPAM hydrogel are illustrated in Figure 4A. The sample with NC-PNIPAM printed next to the midrib (Figure 4A-i) folds on the left with 180° folding angle (Figure 4B), whereas the area without NC-PNIPAM remains flat. On the other hand, the sample where NC-PNIPAM was printed across the midrib (Figure 4A-ii) folds in the center of the decellularized leaf with about 65° folding angle (Figure 4C). The smaller folding angle found in the latter case compared to the former case (Figure 4C vs 4B) can be attributed to the higher Young's modulus of the midrib (976 ± 233 kPa) than the surface (415 ± 98 kPa) of the decellularized leaves as calculated from the stress−strain curves obtained from the tensile test (Figure S2, details can be found in SI). Furthermore, the addition of GO endows the PNIPAM-based system with light responsiveness. To fabricate the GO-NC-PNIPAM/decellularized leaf bilayer structure, the decellularized leaf was cut into a rectangular strip ($10 \times 20 \times 0.1$ mm^3), and the precursor ink was printed on the top to fully cover it (Figure 4D). After photo-cross-linking, the GO-NC-PNIPAM/decellularized leaf bilayer structure was immersed in water at 22 °C to allow the GO-NC-PNIPAM to reach its equilibrium swelling state, at which point the bilayer structure bent (Figure 4E). Upon UV irradiation with an intensity of ∼1 W/cm^2, the structure unbent due to the deswelling by the photothermal effect of GO (Figure 4F, supplementary video S1). In addition, we also printed the GO-NC-PNIPAM across the midrib of the cut decellularized leaf to achieve reversibly folding and unfolding by swelling in a water bath at 22 °C and deswelling upon UV irradiation at an intensity of 1 W/cm^2, respectively (Figure S3, supplementary video S2). We note that the irradiation dose of the applied UV for photoactuation was 1200 kJ/m^{-2}. If this method applies to living plants in the future, this UV dose could damage living plant cells.[30] To avoid this problem, the composition of nanocomposite hydrogels can be further modified to be more sensitive to UV by increasing GO concentration or using different photothermal materials that exhibit higher photothermal efficiency than GO to reduce the UV dose.

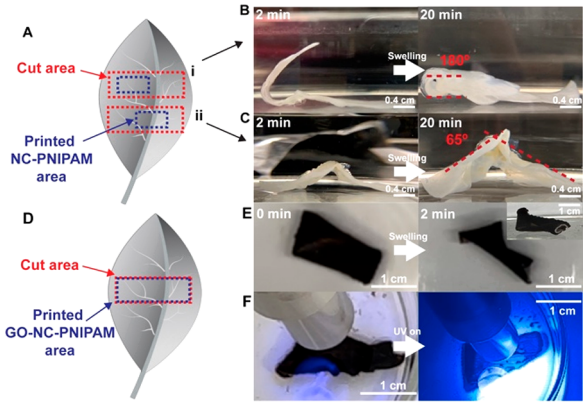

Figure 4. (A) Schematic of the top view of the cut area of the decellularized leaf (red) and NC-PNIPAM (blue) printed (i) on the left-hand side and (ii) across the midrib. Photographs of the side view of the shape-morphing process using the bilayer structures of NC-PNIPAM and silane-treated decellularized leaf during swelling at 23 °C, in which NC-PNIPAM are printed (B) on the left-hand side (correspond to A-i) and (C) across the midrib of the leaves (correspond to A-ii). (D) Schematic showing the cut area of the decellularized leaf (red) and NC-PNIPAM (blue) printed on the top. (E) Top view of the shape morphing process using the bilayer structure of GO-NC-PNIPAM and silane-treated decellularized leaf during swelling at 22 °C and (F) deswelling by UV irradiation at an intensity of ∼1 W/cm^2.

We note that each leaf is different in terms of thickness and mechanical properties, which leads to different folding angles. However, by tuning the thickness and pattern of nanocomposite PNIPAM hydrogels as a swellable part, it is possible to systematically control the folding angle.[20] The programmable shape morphing behavior would be a desired trait for living plants as it offers possibilities to adapt to environmental changes once could be programmed to collapse and fold to hold water and thus prevent surface water evaporation.[31] Plants already achieve this as a natural property in the circadian cycle: during the day leaves spread out to catch sunlight (for photosynthesis), but also to absorb water or catch water from rain; at night the leaves close-up inward to prevent water evaporation and to funnel water collected on the leaves toward the roots of the plants.[32]

In conclusion, we have developed plant-based soft actuators by combining temperature-responsive (NC-PNIPAM) and temperature- and light-responsive (GO-NC-PNIPAM) nanocomposite hydrogels with silane-treated decellularized leaves. We modified and characterized the rheological properties of NC-PNIPAM precursors to enable extrusion-based 3D printing such that they can be printed into the prescribed shapes and spatial locations, where localized strain-mismatch can be induced between the swellable nanocomposite PNIPAM hydrogels and the nonswellable decellularized leaves, resulting in controllable shape morphing. Strong adhesion (adhesion strength >76 ± 7 kPa) has been realized by chemically anchoring the PNIPAM onto the surfaces of

https://doi.org/10.1021/acsmacrolett.2c00282
ACS Macro Lett. 2022, 11, 961−966

decellularized leaves using functional silane. Utilizing the photothermal effect of GO, we successfully demonstrated the UV light responsiveness of the bilayer structure of GO-NC-PNIPAM and the silane-treated decellularized leaf, which endows the structure with remote control ability. Furthermore, different types of out-of-plane deformations (i.e., folding and bending) were achieved by designing the printed pattern of the nanocomposite PNIPAM hydrogels. We note that the approach we developed in this work could presumably be applicable to different stimuli-responsive materials and plant tissues. For example, conductive thermoresponsive[33] and magnetic[34] hydrogels by modifying the PNIPAM composition can serve as good candidates. Plant tissues such as mint or *Arabidopsis* leaves might be a suitable choice because they possess similar characteristics with spinach leaves, such as being relatively flat and soft and having smooth (i.e., less hairy) surfaces. We believe that our work would contribute to the development of plant cyborg concepts that could further push agriculture development and potentially find applications in plant-based soft actuators and robots.

■ ASSOCIATED CONTENT

Supporting Information

The Supporting Information is available free of charge at https://pubs.acs.org/doi/10.1021/acsmacrolett.2c00282.

Experimental details on materials, preparation of nanocomposite hydrogels, decellularization, silane treatment of decellularized spinach leaves, 3D printing process and characterization; tensile test results of nanocomposite hydrogels and decellularized leaves (surface and midrib), as well as characterization of UV responsiveness of GO-NC-PNIPAM/decellularized leaf (PDF)

Video S1: GO-NC-PNIPAM/decellularized leaf bilayer structure unbending upon UV irradiation (MP4)

Video S2: GO-NC-PNIPAM/decellularized leaf bilayer structure folding and unfolding in 23 °C water bath and upon UV irradiation, respectively (MP4)

■ AUTHOR INFORMATION

Corresponding Authors

Nicole F. Steinmetz − *Department of NanoEngineering, University of California San Diego, La Jolla, California 92093, United States; Center for Nano-ImmunoEngineering, Institute for Materials Discovery and Design, Department of Bioengineering, Department of Radiology, and Moores Cancer Center, University of California San Diego, La Jolla, California 92093, United States*; Email: nsteinmetz@ucsd.edu

Jinhye Bae − *Department of NanoEngineering, University of California San Diego, La Jolla, California 92093, United States; Chemical Engineering Program, Material Science and Engineering Program, and Sustainable Power and Energy Center (SPEC), University of California San Diego, La Jolla, California 92093, United States*; orcid.org/0000-0002-2536-069X; Email: j3bae@ucsd.edu

Authors

Jiayu Zhao − *Department of NanoEngineering, University of California San Diego, La Jolla, California 92093, United States*

Yifeng Ma − *Department of NanoEngineering, University of California San Diego, La Jolla, California 92093, United States*

Complete contact information is available at: https://pubs.acs.org/10.1021/acsmacrolett.2c00282

Notes

The authors declare no competing financial interest.

■ ACKNOWLEDGMENTS

This work was supported by the National Science Foundation through the University of California San Diego Materials Research Science and Engineering Center (UCSD MRSEC), Grant Number DMR-2011924.

■ REFERENCES

(1) Nguyen, P. Q.; Courchesne, N.-M. D.; Duraj-Thatte, A.; Praveschotinunt, P.; Joshi, N. S. Engineered Living Materials: Prospects and Challenges for Using Biological Systems to Direct the Assembly of Smart Materials. *Adv. Mater.* **2018**, *30* (19), 1704847.

(2) Chen, A. Y.; Zhong, C.; Lu, T. K. Engineering Living Functional Materials. *ACS Synth. Biol.* **2015**, *4* (1), 8−11.

(3) Liu, X.; Yuk, H.; Lin, S.; Parada, G. A.; Tang, T.-C.; Tham, E.; de la Fuente-Nunez, C.; Lu, T. K.; Zhao, X. 3D Printing of Living Responsive Materials and Devices. *Adv. Mater.* **2018**, *30* (4), 1704821.

(4) Duprey, A.; Chansavang, V.; Frémion, F.; Gonthier, C.; Louis, Y.; Lejeune, P.; Springer, F.; Desjardin, V.; Rodrigue, A.; Dorel, C. NiCo Buster": engineering E. coli for fast and efficient capture of cobalt and nickel. *J. Biol. Eng.* **2014**, *8* (1), 19.

(5) Lee, K. Y.; Park, S.-J.; Matthews, D. G.; Kim, S. L.; Marquez, C. A.; Zimmerman, J. F.; Ardona, H. A. M.; Kleber, A. G.; Lauder, G. V.; Parker, K. K. An autonomously swimming biohybrid fish designed with human cardiac biophysics. *Science* **2022**, *375* (6581), 639−647.

(6) Del Dottore, E.; Sadeghi, A.; Mondini, A.; Mattoli, V.; Mazzolai, B. Toward Growing Robots: A Historical Evolution from Cellular to Plant-Inspired Robotics. *Front. Robot. AI* **2018**, *5*, 16.

(7) Qu, C. C.; Sun, X. Y.; Sun, W. X.; Cao, L. X.; Wang, X. Q.; He, Z. Z. Flexible Wearables for Plants. *Small* **2021**, *17* (50), No. 2104482.

(8) Stavrinidou, E.; Gabrielsson, R.; Gomez, E.; Crispin, X.; Nilsson, O.; Simon, D. T.; Berggren, M. Electronic plants. *Sci. Adv.* **2015**, *1* (10), No. e1501136.

(9) Gordiichuk, P.; Coleman, S.; Zhang, G.; Kuehne, M.; Lew, T. T. S.; Park, M.; Cui, J.; Brooks, A. M.; Hudson, K.; Graziano, A. M.; Marshall, D. J. M.; Karsan, Z.; Kennedy, S.; Strano, M. S. Augmenting the living plant mesophyll into a photonic capacitor. *Sci. Adv.* **2021**, *7* (37), No. eabe9733.

(10) Yu, A. C.; Lopez Hernandez, H.; Kim, A. H.; Stapleton, L. M.; Brand, R. J.; Mellor, E. T.; Bauer, C. P.; McCurdy, G. D.; Wolff, A. J.; Chan, D.; Criddle, C. S.; Acosta, J. D.; Appel, E. A. Wildfire prevention through prophylactic treatment of high-risk landscapes using viscoelastic retardant fluids. *Proc. Natl. Acad. Sci. U.S.A.* **2019**, *116* (42), 20820−20827.

(11) Li, W.; Matsuhisa, N.; Liu, Z.; Wang, M.; Luo, Y.; Cai, P.; Chen, G.; Zhang, F.; Li, C.; Liu, Z.; Lv, Z.; Zhang, W.; Chen, X. An on-demand plant-based actuator created using conformable electrodes. *Nat. Electron.* **2021**, *4* (2), 134−142.

(12) Bao, J.; Hou, C.; Chen, M.; Li, J.; Huo, D.; Yang, M.; Luo, X.; Lei, Y. Plant Esterase-Chitosan/Gold Nanoparticles-Graphene Nanosheet Composite-Based Biosensor for the Ultrasensitive Detection of Organophosphate Pesticides. *J. Agric. Food Chem.* **2015**, *63* (47), 10319−10326.

(13) Harris, A. F.; Lacombe, J.; Zenhausern, F. The Emerging Role of Decellularized Plant-Based Scaffolds as a New Biomaterial. *Int. J. Mol. Sci.* **2021**, *22* (22), 12347.

(14) McCulloh, K. A.; Sperry, J. S.; Adler, F. R. Water transport in plants obeys Murray's law. *Nature* **2003**, *421* (6926), 939−942.
(15) Walawalkar, S.; Almelkar, S. Fabricating a pre-vascularized large-sized metabolically-supportive scaffold using Brassica oleracea leaf. *J. Biomater. Appl.* **2021**, *36* (1), 165−178.
(16) Gershlak, J. R.; Hernandez, S.; Fontana, G.; Perreault, L. R.; Hansen, K. J.; Larson, S. A.; Binder, B. Y. K.; Dolivo, D. M.; Yang, T.; Dominko, T.; Rolle, M. W.; Weathers, P. J.; Medina-Bolivar, F.; Cramer, C. L.; Murphy, W. L.; Gaudette, G. R. Crossing kingdoms: Using decellularized plants as perfusable tissue engineering scaffolds. *Biomaterials* **2017**, *125*, 13−22.
(17) Modulevsky, D. J.; Lefebvre, C.; Haase, K.; Al-Rekabi, Z.; Pelling, A. E. Apple Derived Cellulose Scaffolds for 3D Mammalian Cell Culture. *PLoS One* **2014**, *9* (5), No. e97835.
(18) Hickey, R. J.; Modulevsky, D. J.; Cuerrier, C. M.; Pelling, A. E. Customizing the Shape and Microenvironment Biochemistry of Biocompatible Macroscopic Plant-Derived Cellulose Scaffolds. *ACS Biomater. Sci. Eng.* **2018**, *4* (11), 3726−3736.
(19) Fujishige, S.; Kubota, K.; Ando, I. Phase transition of aqueous solutions of poly(N-isopropylacrylamide) and poly(N-isopropylmethacrylamide). *J. Phys. Chem.* **1989**, *93* (8), 3311−3313.
(20) Zhao, J.; Bae, J. Microphase Separation-Driven Sequential Self-Folding of Nanocomposite Hydrogel/Elastomer Actuators. *Adv. Funct. Mater.* **2022**, *32*, 2200157.
(21) Li, M.; Bae, J. Tunable swelling and deswelling of temperature- and light-responsive graphene oxide-poly(N-isopropylacrylamide) composite hydrogels. *Polym. Chem.* **2020**, *11* (13), 2332−2338.
(22) Tang, L.; Wang, L.; Yang, X.; Feng, Y.; Li, Y.; Feng, W. Poly(N-isopropylacrylamide)-based Smart Hydrogels: Design, Properties and Applications. *Prog. Mater. Sci.* **2021**, *115*, 100702.
(23) Haraguchi, K.; Takehisa, T. Nanocomposite Hydrogels: A Unique Organic-Inorganic Network Structure with Extraordinary Mechanical, Optical, and Swelling/De-swelling Properties. *Adv. Mater.* **2002**, *14* (16), 1120−1124.
(24) Siacor, F. D. C.; Chen, Q.; Zhao, J. Y.; Han, L.; Valino, A. D.; Taboada, E. B.; Caldona, E. B.; Advincula, R. C. On the additive manufacturing (3D printing) of viscoelastic materials and flow behavior: From composites to food manufacturing. *Addit. Manuf.* **2021**, *45*, 102043.
(25) Dugas, V.; Chevalier, Y. Surface hydroxylation and silane grafting on fumed and thermal silica. *J. Colloid Interface Sci.* **2003**, *264* (2), 354−361.
(26) Kang, H.-W.; Tabata, Y.; Ikada, Y. Fabrication of porous gelatin scaffolds for tissue engineering. *Biomaterials* **1999**, *20* (14), 1339−1344.
(27) Yuk, H.; Varela, C. E.; Nabzdyk, C. S.; Mao, X.; Padera, R. F.; Roche, E. T.; Zhao, X. Dry double-sided tape for adhesion of wet tissues and devices. *Nature* **2019**, *575* (7781), 169−174.
(28) Cai, S.; Suo, Z. Mechanics and chemical thermodynamics of phase transition in temperature-sensitive hydrogels. *J. Mech. Phys. Solids* **2011**, *59* (11), 2259−2278.
(29) Yang, Z.; Yang, X.; Long, R.; Li, J. Stimulation Modulates Adhesion and Mechanics of Hydrogel Adhesives. *Langmuir* **2021**, *37* (23), 7097−7106.
(30) Bosshard, F.; Riedel, K.; Schneider, T.; Geiser, C.; Bucheli, M.; Egli, T. Protein oxidation and aggregation in UVA-irradiated Escherichia coli cells as signs of accelerated cellular senescence. *Environ. Microbiol.* **2010**, *12* (11), 2931−2945.
(31) Ahmad, H.; Sehgal, S.; Mishra, A.; Gupta, R. Mimosa pudica L. (Laajvanti): An overview. *Pharmacogn Rev.* **2012**, *6* (12), 115−124.
(32) McClung, C. R. Plant circadian rhythms. *Plant cell* **2006**, *18* (4), 792−803.
(33) Jia, M.; Zhang, J. Thermoresponsive PEDOT:PSS/PNIPAM conductive hydrogels as wearable resistive sensors for breathing pattern detection. *Polym. J.* **2022**, *54* (6), 793−801.
(34) Purushotham, S.; Ramanujan, R. V. Thermoresponsive magnetic composite nanomaterials for multimodal cancer therapy. *Acta Biomater.* **2010**, *6* (2), 502−510.

https://doi.org/10.1021/acsmacrolett.2c00282
ACS Macro Lett. 2022, 11, 961−966